Building and Environment 251 (2024) 111211

Contents lists available at ScienceDirect

Building and Environment

journal homepage: www.elsevier.com/locate/buildenv

A holistic two-stage decision-making methodology for passive and active building design strategies under uncertainty

Chujun Zong [a,*], Xia Chen [b], Fatma Deghim [a], Johannes Staudt [a], Philipp Geyer [b], Werner Lang [a]

[a] Institute of Energy Efficient and Sustainable Design and Building, Technical University of Munich, Arcisstraße 21, Munich, 80333, Germany
[b] Sustainable Building Systems, Leibniz University Hannover, Herrenhäuser Straße 8, Hannover, 30419, Germany

ARTICLE INFO

Keywords:
Passive design
Life cycle assessment
Decision-making
Multi-objective optimization
Uncertainty
Two-stage stochastic programming
Machine learning

ABSTRACT

In the last decade, many studies focused on finding optimal design solutions considering trade-offs between different aspects of building design. Accordingly, multi-objective optimization (MOO) approaches have been increasingly applied in the building industry. However, certain aspects must be deepened to ensure a more effective decision-making process in the early planning phase. On the one hand, uncertainties should be considered before making decisions to ensure the robustness of the optimal solutions; on the other hand, decisions are made at different times in building planning, and the sequential order of making decisions should be modeled. This paper presents a holistic *two-stage multi-objective stochastic optimization (MOSO)-II framework* to minimize the environmental impact of global warming potential (GWP) and cost throughout the entire life cycle of a building (phases of A1-A3, B4, B6 and C3-C4), considering passive and active design strategies in two consecutive stages, under uncertainty. Herein, individual/use and political/market uncertainties are considered. As a proof of concept, the proposed framework is applied in a case study for a generic zone in a multi-family terraced residential building type with solid brick construction. The advantages of the proposed framework are validated by comparing it with alternative single-stage MOSO frameworks. Results show that the proposed *two-stage MOSO-II framework* can deliver a smaller range of solutions with a better performance in terms of lower GWP and cost. It indicates that the proposed framework can effectively assist planners in decision-making by reducing the effort in choosing the proper solution. Secondly, the results also emphasize the importance of passive design strategies in sustainable building planning. In addition, the energy mix structure and cost of energy sources should be carefully adjusted in the future to promote a more ecologically sustainable building design.

1. Introduction

1.1. Background

Thanks to more advanced computer-aided technologies, such as building information modeling (BIM), design solutions can be assessed and adjusted in the design phase of a building, avoiding potential financial and personnel efforts of later changes [1]. During the decision-making process, different objectives should be considered. In the building industry, the most commonly considered objectives include operational energy consumption, thermal comfort, daylight conditions, environmental impact through life cycle impact assessment (LCIA) and economic impact through life cycle cost (LCC) analysis [2]. Nevertheless, certain objectives are conflicting which makes it difficult to determine an optimal solution [3]. Thus, aiming at finding the optimal solutions considering trade-offs between the conflicting objectives in the early decision-making process, multi-objective optimization (MOO) approaches are introduced. Accordingly, instead of one unique optimal solution, a set of Pareto-optimal solutions can be obtained as a solution catalogue.

In the last decade, owing to the rapid development of multi-objective evolutionary algorithms, an increasing number of studies has been conducted to investigate MOO problems with different objectives in the building industry. In this context, the research focus is on environmental impacts and energy consumption embedded in building materials and during building operation, as well as investment and operational cost. Using non-dominated sorting genetic algorithm II (NSGA-II) [4], Azari et al. [5] thoroughly investigated the synergistic effects of common indicators to evaluate environmental impacts. Herein, operational energy consumption was obtained through dynamic building simulation using eQuest and a subsequent machine intelligence approach. Abdou et al. [6] identified net-zero energy

* Corresponding author.
E-mail address: chujun.zong@tum.de (C. Zong).

https://doi.org/10.1016/j.buildenv.2024.111211
Received 4 November 2023; Received in revised form 4 January 2024; Accepted 12 January 2024
Available online 13 January 2024

building solutions taking into account global warming potential (GWP) and LCC. In [7], the attention of Ciardiello et al. is directed towards GWP, energy consumption and cost during building operation, as well as investment cost, with geometry configuration considered as design variables. In more recent studies, the research focus has been shifted to occupant comfort. In [8], Gagnon et al. realized a holistic design framework aiming at reducing carbon footprint and LCC, as well as improving thermal comfort. Similarly, Chang et al. [9] studied trade-offs among energy consumption, predicted discomfort, GWP, LCC and payback period. Moreover, there has been a growing interest in visual comfort, as well [10–12].

Despite the increasing breadth of research areas, there is still a lack of thorough investigation on certain aspects of MOO approaches to enhance the effectiveness of real-world decision-making processes for a building design. One of the most important issues affecting the reliability of optimization problem results in decision-making is the uncertainty arising due to incomplete data or knowledge about the accurate values of certain variables [13]. Studies have been conducted to analytically investigate uncertainties in building geometry [7,14,15], building materials [16–20], internal heat gain [21] and operational energy consumption [22]. Among all, sensitivity analysis and uncertainty analysis are the most widely applied methodologies. Particularly in MOO problems, sensitivity and uncertainty analyses can both serve as a post-results evaluation of different design decisions subject to uncertainties. For instance, Mukkavaara and Shadram [23] applied sensitivity analysis to evaluate different design decisions while weighing the trade-offs between operational and embedded energy consumption.

However, as a tool primarily for analysis and evaluation, both sensitivity and uncertainty analyses are constrained when directly integrating uncertainties in decision-making processes. Studies show that it is common to utilize temporary materials as placeholders during initial design phases while using modeling software, such as BIM [24]. As a result, arbitrary selections of these temporary materials may result in a less substantial design aid for simulating operational energy consumption, as well as for conducting an LCIA calculation and investment cost analysis based on the building model's Bill of Quantities [24]. To address this issue, [25–27] developed structured life cycle inventories with hierarchical categorization of building component assembly possibilities. This approach enables a fast LCIA calculation and a presentation of all possible design solutions in early design phases. However, the wide range of possible design solutions in early design phases could be potentially reduced to ease the actual decision-making process. Thus, it is of interest to integrate uncertainties in optimization processes early to effectively influence decision-making and attain potentially more robust optimal design solutions. Hester et al. [28] investigated the quasi-optimal region of achieving possibly low LCIA and cost by using genetic optimization. Galimshina et al. [29] incorporated material and environmental uncertainties into the MOO approach using robust optimization with a surrogate-assisted Kriging model. Subsequently, the most cost-efficient and environmental profitable retrofit solutions could be achieved. Liu et al. [30] investigated the impacts of climate uncertainties on building energy consumption by generating climate scenarios and applying stochastic programming. In [20], Zong et al. proposed a multi-objective stochastic optimization framework to assist decision-making in the early design phase of building façade while considering GWP and LCC. Herein, environmental uncertainties and uncertainty in design decisions were included in a MOO problem through stochastic programming. Similarly, in [31], multi-objective stochastic optimization was utilized to properly size energy systems considering economic and environmental influences, as well as thermal comfort. The increasing number of studies in the building industry applying stochastic programming in MOO problems indicates the rationale and benefits of this method when integrating uncertainty prior to making decisions.

Another issue in the decision-making process with regard to building design is that different design decisions of different decision stages should be taken into account. In sustainable building planning, design strategies can be categorized into passive and active strategies [32]. While the former focuses on improving building envelope, structure, surfaces, geometry, orientation, etc., the latter refers to building technological measures, such as heating, ventilation, and air-conditioning (HVAC) systems. In the past decade, many studies have been conducted to analyze passive and active strategies [33–36]. In [37], the finding indicates the dependency of passive and active design strategies and suggests a holistic consideration of both strategies while investigating energy-efficient and environmentally friendly design solutions. Accordingly, in more recent studies, passive and active design strategies have been more often integrated into MOO problems. For instance, [7] considered active and passive strategies as design variables in the defined MOO problem. However, in real-world decision-making problems of building design, passive and active decisions are often made at different points in time and the sequential order should be modeled to ensure a higher reliability of the decision-making process. Some studies used stage optimization to optimize different objectives. Hamdy et al. [38] proposed a three-stage MOO approach to find optimal design decisions considering trade-offs between energy consumption and cost. However, the defined optimization stages do not correspond to real-world decision stages. In addition, no uncertainty is mathematically integrated into optimization problems. In [39], Xu et al. split the optimization process into building envelope development and energy generation system optimization. However, the optimization problem does not consider uncertainty and the separation of design phases is realized through manual means rather than mathematical methods, which can lead to cumbersome implementation procedures.

1.2. The aim of the study

Mathematically, multi-stage stochastic programming can be applied to solve optimization problems containing different decision stages while considering uncertainty. While this method has been implemented in other fields to model the decision-making process, such as for energy system management [40,41], it still needs further investigation in building planning. Hence, this paper develops a holistic multi-objective stochastic decision-making framework with passive and active design strategies segmented into two stages, while considering uncertainty. The proposed framework aims to identify the optimal environmentally friendly and economical design strategies that can withstand various uncertainties and thus maintain a high level of robustness. The main focus of this study includes the followings:

- presentation of a *two-stage multi-objective stochastic optimization framework* for finding the optimal robust building design solutions,
- defining passive and active design strategies as two decision stages in building planning,
- targeting at minimum life cycle environmental impact and cost in the optimization problem,
- integration of uncertainties in the decision-making process for early design phases through stochastic programming,
- comparison of the established framework with alternative single-stage multi-objective stochastic optimization approaches.

2. Methodology

The methodological workflow of the presented study is illustrated in Fig. 1. Design variables are derived from a knowledge-based database, from which specific intermediate inputs are extracted and fed into a machine learning model to obtain operation energy consumption. Through the proposed *two-stage multi-objective stochastic optimization (MOSO-II) framework*, the possibly most robust and optimal design solutions for passive and active strategies can be obtained while considering uncertainties.

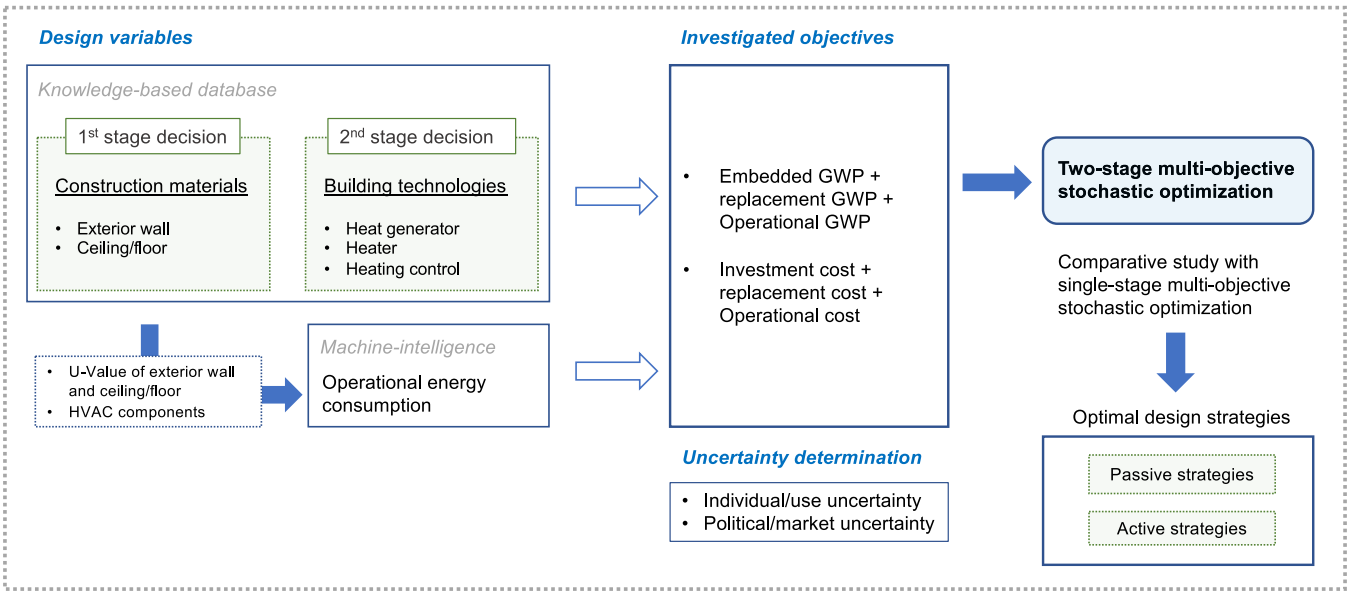

Fig. 1. Methodological workflow of the paper.

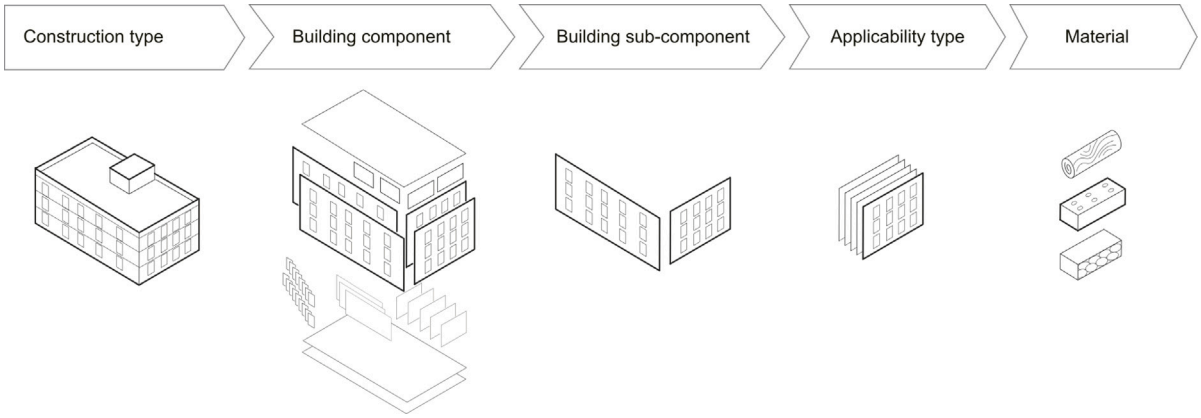

Fig. 2. Knowledge-based database for building materials [27].

2.1. Data basis of the study

An expert-knowledge-assisted database was created and utilized as the foundational data source for the proposed framework, facilitating a systematic way of extracting case-specific design variables of building materials [27,42]. As illustrated in Fig. 2, the data structure contains levels of building component (e.g., exterior wall), building sub-component, applicability type (e.g., wall cladding) and material. Herein, building sub-components are defined according to the German DIN 276 [43]. The assembly possibilities of applicability types within each sub-component are defined based on expert knowledge from architects and can differ for different construction types. In total, four construction types are defined: timber, brick, reinforced concrete and steel construction.

In the bottom layer of the database, different materials are assigned with relevant information, including life cycle impact assessment (LCIA) unit data, thickness-related unit investment cost based on [44,45], thermal conductivity (λ-value), as well as reference service life (RSL) based on [46,47] and thickness ranges of materials for different applicability types. The LCIA unit data are modeled based on EN-15978 [48] and extracted from the standardized foreground database ÖKOBAUDAT [49], published by the Federal Ministry for Housing, Urban Development and Building. Although various evaluation indicators are included in ÖKOBAUDAT, only global warming potential (GWP) is preliminarily included in the knowledge-based database to test its feasibility. As building materials mainly contribute to the embedded environmental impacts in the LCIA calculation procedure, the established database contains LCIA unit data covering modules of product (A1-A3), disposal (C3-C4) and replacement (B4) that is expressed as the replacement frequency calculated based on the defined reference study period and individual RSLs. In addition, to ensure the consistency in functional units, all materials are investigated based on volume (1 m^3). Subsequently, the material thickness is determined by the thickness of the materials that are in or transformed into 1 m^2.

As for building technologies, heating, mechanical ventilation and air-conditioning (HVAC) components are individually considered. For instance, three components are included in heating systems: heat generator, heater and heating control system. Based on the proposed methodology from [50,51], HVAC components are assigned with LCIA unit data based on ÖKOBAUDAT, investment cost based on [44], possible auxiliary components, and individual RSLs. For the LCIA unit data, besides modules of A1-A3, C3-C4 and B4, GWP values of module B6 indicating the CO_2 emissions during operation are included. Correspondingly, different energy prices are included as well.

2.2. Design strategies and decision stages

As aforementioned, the goal of the established *two-stage multi-objective stochastic optimization (MOSO-II) framework* is to model a

holistic two-stage decision-making process to find the possibly most robust passive and active design strategies considering trade-offs between environmental impacts and costs. In the following, investigated design strategies and decision stages in this paper are introduced.

As defined by [32], to achieve energy-efficient and environmentally friendly goals, building design decisions can be classified into two categories: passive and active strategies. Passive strategies refer to measures without actively using additional energy input, such as the improvement of building envelope materials, building geometry, orientation, etc. In this paper, the choice of building materials is exemplarily considered as passive design strategies. On the other hand, active strategies refer to measures that use and produce additional energy actively. Accordingly, HVAC systems fall into this category. While some studies treat passive and active strategies as equally weighted variables that are examined simultaneously, in actual decision-making processes, passive strategies are often determined prior to active strategies. In extreme built cases [52,53], highly functional passive design strategies can affect active strategies such that HVAC systems are barely needed. Thus, the sequential order of the two strategies in the decision-making process should be modeled. In this context, the decision-making process should be divided into two stages. The first-stage decisions are alternatively determined as "here-and-now" decisions and the second-stage decisions are also known as "recourse" or "wait-and-see" decisions. While the former decisions need to be made prior to knowing the realized uncertainty parameters, the latter decisions depend on the first-stage decisions and uncertainties [40]. In this paper, decisions in two stages are specifically defined as follows:

- The **first-stage decisions** describe the passive design strategies, i.e., the choice of building component materials and the corresponding thickness.
- The **second-stage decisions** refer to active design strategies, i.e., the choice of HVAC system components.

2.3. Design variables and objectives

Using the described data source of this study, design variables can be extracted systematically. Design variables for first-stage decisions refer to building materials. Specifically, two types of variables are included: categorical and continuous variables, representing the material choice for each applicability type and the corresponding thickness. As for second-stage decisions, only categorical variables are considered for different HVAC components. It is to note that auxiliary components, e.g., piping and tanks of heating systems, are not considered as design variables but additional elements belonging to certain HVAC components with individual RSLs.

The two targeted objectives in the optimization problem are minimizing total GWP throughout the whole building life cycle and life cycle cost (LCC).

Aiming at minimizing the total GWP throughout the whole building life cycle,

- the stage objective of the **first-stage decisions** is the embedded GWP of building materials;
- the stage objective of the **second-stage decisions** is the embedded GWP of HVAC system components and GWP during building operation for defined reference study period.

As for the second objective,

- the stage objective of the **first-stage decisions** is the investment cost of building materials;
- the stage objective of the **second-stage decisions** is the investment cost of HVAC system components and energy cost during building operation for defined reference study period.

In total, the examined life cycle phases are comprised of the modules A1-A3, B4, B6 and C3-C4.

2.4. Uncertainty determination

In decision-making processes, especially during early planning stages, uncertainty stems from incomplete data or inadequate knowledge regarding precise values of specific variables [13]. In this paper, two kinds of uncertainty are considered: individual/use uncertainty and political/market uncertainty. The former refers to the uncertain actual operational energy consumption despite similar active and passive design strategies. According to different studies [54,55], the distribution of operational heating energy consumption of residential buildings gradually approaches a normal distribution as dwelling number rises, reflecting the diversity in occupant's sensation of thermal comfort and behavior of adjusting HVAC systems according to uncertain microenvironmental conditions. In addition, this uncertainty is also partially due to the actual energy efficiency of the active systems. In the presented study, the individual/use uncertainty is taken into account in obtaining operational energy consumption through a machine assistance approach (see 2.5) given inputs of thermal transmittance (U-value) of building components and HVAC components.

Regarding the second uncertainty, energy prices are susceptible to fluctuations in response to alterations in political conditions and market volatility. Thus, political/market uncertainty is reflected in the uncertain inflation rate of energy prices subject to different energy sources. It is derived from the analysis of the development of energy prices from 2008 to the first half of 2022 in Germany, based on the data from the federal statistical office of Germany [56] and the statistical office of the European Union Eurostat [57].

2.5. Machine assistance

As module B6 is considered in the second-stage decisions, the analysis of operational energy consumption is required. For this purpose, a machine assistance approach is used. In the last decade, machine learning approaches have been widely used to estimate operational energy consumption given specific inputs in order to reduce the computational effort of dynamic building simulations [58]. In this study, we use the machine learning approach used in the previously established machine assistance framework from [59].

Using the Natural Gradient Boosting (NGBoost) algorithm [60], the machine assistance approach offers a nervous-inspired uncertainty quantification pipeline to pinpoint probabilistic relationships within data-driven behavior through surrogate modeling. To effectively incorporate uncertainties into surrogate modeling, probabilistic regression is utilized given its capacity to produce a comprehensive distribution over the outcome space, conditioned on the inputs. This multi-parameter boosting algorithm extends the gradient boosting framework to facilitate probabilistic regression by treating the parameters of the conditional distribution as target variables. In contrast to point prediction, which involves comparing observed data using a loss function, probabilistic regression employs a scoring rule (e.g., negative log-likelihood) as its objective. It compares the estimated probability distribution to the observed data for validation purposes and identifies the uncertainties in a dataset.

For the dataset, we use the real-world, open-sourced Energy Performance of Buildings Data: England and Wales [61]. The domestic Energy performance certificate (EPC) is chosen as it contains a building feature dataset with representative properties of a building that are relevant in the early stages, such as conceptual design parameters, including geometry, building component properties, and energy system description. In this study, the dataset is used for a rough estimation of operational energy consumption in geographical areas with the same Köppen-Geiger climate classification of "Cfb" [62,63].

With the machine assistance approach, the total operational primary energy consumption of an entire housing unit is obtained given the previously mentioned design variables of active and passive design strategies. This includes HVAC components and the U-value of investigated building components, which is calculated based on material choices for investigated applicability types and the corresponding thickness.

2.6. Two-stage multi-objective stochastic optimization

The established MOSO-II framework is based on stochastic programming to model uncertainties. Generally, a stochastic programming model can be presented as follows:

$$\min_{x\in X, X\in\mathbb{R}^m, \xi\in\mathbb{R}^n} \{F(x) := \mathbb{E}_P[f(x,\xi)]\} \tag{1}$$

where $F(x)$ is the expected value (EV) function of the problem corresponding to the true value function $f(x,\xi)$ containing the random vector ξ representing the uncertainty parameter [64]. It is to note that the probability distribution P of each random vector ξ should be priorly known. In problems with discrete interpretation, i.e., discrete scenarios with the corresponding probabilities, the EV function can be formed as:

$$\mathbb{E}_P[f(x,\xi)] = \sum_{k=1}^{N} p_k f(x,\xi_k). \tag{2}$$

where ξ_k represents the uncertainty parameter in the k^{th} scenario with the corresponding probability p_k. Scenarios and corresponding probabilities are to be predefined, for instance, based on analytical studies of historical data.

However, when the scenario generation becomes relatively complex and in order to reduce the computational effort of applying Eq. (2), the approximated true value can be obtained using the exterior Monte Carlo (MC) sampling approach [64]. By drawing N pseudo-random samples of ξ_k from a known probability distribution function (PDF) P, the EV function of Eq. (1) can be approximated using Eq. (3):

$$\min_{x\in X, X\in\mathbb{R}^m, \xi\in\mathbb{R}^n} \{\hat{F}_N(x) := \frac{1}{N}\sum_{k=1}^{N} f(x,\xi_k)\} \tag{3}$$

which is called the sample average approximation (SAA) approach [64,65]. According to the Law of Large Numbers, $\hat{F}_N(x)$ in Eq. (3) can approximate F_x in Eq. (1) if N is infinitely close to ∞ [64]. Based on the results of previous work [20], the sample size N is determined as 1000 in this paper to reduce the computational cost while achieving a possibly satisfactory approximation.

In this work, depending on different uncertainty parameters, Eq. (2) and Eq. (3) are selectively applied such that a stochastic programming problem can be transformed into a deterministic optimization problem and be solved.

When integrating two-stage decisions in stochastic programming, the model is denoted as [66]:

$$\min_{x\in X} \quad C^\top x + \mathbb{E}_P[Q(x,\xi)] \tag{4}$$

through which the decision-making process is divided into two stages. While the whole decision-making process is optimized holistically, the second-stage decision is influenced by the first-stage decision. $C^\top x$ represents the first-stage decision process and $\mathbb{E}_P[Q(x,\xi)]$ represents the second-stage decision. Herein, $Q(x,\xi)$ is the optimization problem, where x corresponds to the design variable derived from first-stage decisions, and ξ represents the uncertainty parameter. It is defined as follows:

$$\begin{aligned} &Q(x,\xi) = \min_y q(\xi)^\top y \\ &s.t. \quad W(\xi)y + T(\xi)x \le s(\xi) \end{aligned} \tag{5}$$

where y stands for the design variable of the second-stage decisions.

In the context of this work, based on the afore-defined passive and active design strategies as well as decision stages for buildings, the MOSO-II problem is denoted as:

$$\begin{aligned} &\min_{y\in Y, \xi\in\mathbb{R}} \quad \sum_{i=1}^{N} G_c(k_i) + \mathbb{E}_P[\sum_{j=1}^{J} G_{oe}(y_j) + G_o(y, u(k_i), \xi_o)] \\ &\min_{y\in Y, \xi\in\mathbb{R}} \quad \sum_{i=1}^{N} C_c(k_i) + \mathbb{E}_P[\sum_{j=1}^{J} C_{oe}(y_j) + C_o(y, u(k_i), \xi_c, \xi_o)] \\ &s.t. \quad u(k_i) \le U \end{aligned} \tag{6}$$

where G_c stands for embedded GWP of building materials representing the **first-stage decisions**. k_i is the variable set of the i^{th} building component containing the categorical design variable x_m and the continuous design variable d_m, representing the material choice and the corresponding thickness of the applicability type in the m^{th} order, as shown in equation decomposition in Eq. (8) and Eq. (9).

As for the active strategies, i.e., **second-stage decisions**, the expected value function of the true value functions G_{oe} and G_o are defined. G_{oe} represents embedded GWP of HVAC system components, whilst G_o represents the GWP during building operation. Herein, y_j is the categorical variable referring to the investigated HVAC components. Uncertainty parameters of operational energy and energy price are expressed as ξ_o and ξ_c, respectively.

In addition, $u(k_i)$ is the cumulative U-value of each building component and is constrained by the predefined value according to different energy standards. Within the framework of this work, the German Building Energy Act (GEG) and Nearly Zero Energy Building (NZEB) standard are considered. Correspondingly, the constrained U-value of exterior walls for the two standards is 0.21 and 0.18 W/m^{2}K, respectively. Specifically, the U-value of each building component is obtained through the thermal resistance (R-value) of each material of the respective applicability type, which is calculated through $\frac{d_m}{lmd(x_m)}$, with lmd representing the λ-value of the investigated materials. Accordingly, $u(k_i)$ can be calculated as follows:

$$u(k_i) = \frac{1}{R_{se} + \sum_{m=1}^{M} \frac{d_m}{lmd(x_m)} + R_{si}}, \quad x\in X, d\in D \tag{7}$$

The second function in Eq. (6) is defined in a similar manner. C_c refers to the investment cost of building materials, while C_{oe} and C_o stand for investment and operational cost of HVAC systems, respectively.

In detail, the equation decomposition of functions in Eq. (6) is shown below. For first-stage decisions, the calculation of the GWP of building materials is shown in Eq. (8):

$$G_c(k_i) = A_i \cdot \sum_{m=1}^{M} g_e(x_m)\cdot d_m \cdot \frac{t}{l(x_m)}, \quad x\in X, d\in D \tag{8}$$

where g_e is the unit embedded GWP value of each material x_m of the m^{th} applicability type and is expressed as a function of it. The unit LCIA value of embedded GWP is multiplied with the corresponding thickness d_m of the material and the frequency of replacement, which is denoted as $\frac{t}{l(x_m)}$. Herein, t is the reference study period and l is the RSL of each material. While applicability types are the categorical design variables, the corresponding thickness is the continuous variable. Subsequently, the embedded GWP of all applicability types in the investigated building component are summed up and multiplied with the area of the building component A_i. Similarly, the cost of passive design strategies is calculated as shown in Eq. (9). Instead of the unit embedded GWP value, the unit investment cost value c_e is utilized.

$$C_c(k_i) = A_i \cdot \sum_{m=1}^{M} c_e(x_m, d_m)\cdot d_m \cdot \frac{t}{l(x_m)}, \quad x\in X, d\in D \tag{9}$$

For the embedded GWP of HVAC components of the second-stage decisions, as shown in Eq. (10), two parts are taken into account: the main component y_j and the case-specific auxiliary components $a(y_j)$ depending on different systems. For instance, the heating system incorporates a liquid petroleum gas (LPG) tank, with the main component being an LPG-driven boiler.

$$G_{oe}(y_j) = g_e(y_j)\cdot\frac{t}{l(y_j)} + g_e(a(y_j))\cdot\frac{t}{l(a(y_j))}, \quad y\in Y \tag{10}$$

To calculate the GWP during the operational phase with active design strategies, operational energy O, in which the individual/use

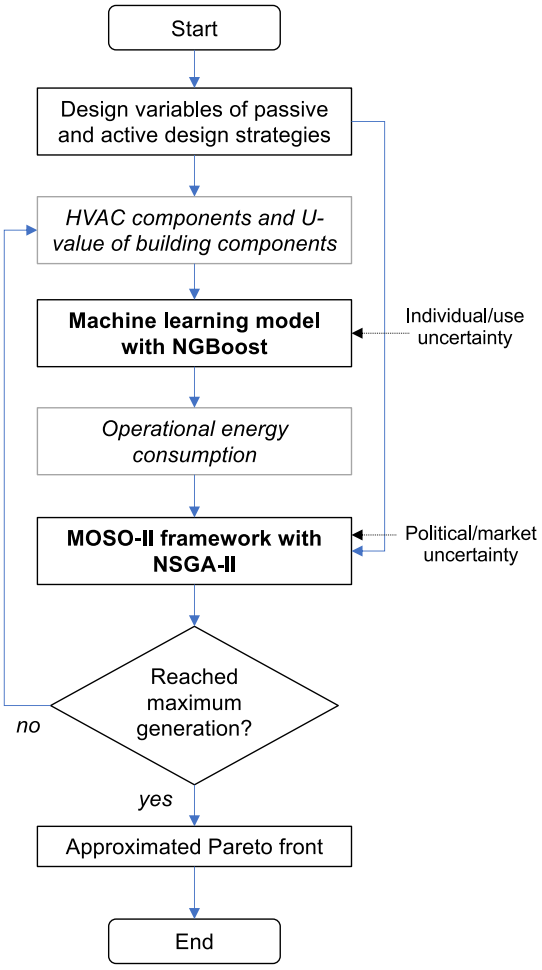

Fig. 3. Workflow of the MOSO-II framework.

uncertainty ξ_o is contained, is obtained as an output from the machine assistance model. This is achieved by providing inputs of the HVAC component set y and the U-value of the specific building component $u(k_i)$. Since use energy is required to match the unit GWP value from the knowledge-based database [27,49], the obtained primary energy consumption from the machine learning model is additionally converted to use energy by being divided by the system efficiency factor of each boiler according to DIN V-4701-10 [67]. Herein, it is assumed that 62.8% refers to heating based on [68]. Accordingly, the operational GWP is denoted as Eq. (11):

$$G_o(y, u(k_i), \xi_o) = g_o(y) \cdot O(y, u(k_i), \xi_o) \cdot t \cdot A_f, \quad y \in Y \tag{11}$$

where g_o is the unit GWP value during operation, t is the reference study period and A_f represents the floor area. As for the calculation of LCC of active strategies, the calculation of investment and operational cost of HVAC systems is shown in Eq. (12) and Eq. (13), respectively. In the calculation of operational cost, uncertainty scenarios of energy prices ξ_c are included additionally.

$$C_{oe}(y_j) = c_e(y_j) \cdot \frac{t}{l(y_j)} + c_e(a(y_j)) \cdot \frac{t}{l(a(y_j))}, \quad y \in Y \tag{12}$$

$$C_o(y, u(k_i), \xi_o) = c_o(y, \xi_c) \cdot O(y, u(k_i), \xi_o) \cdot t \cdot A_f, \quad y \in Y \tag{13}$$

The established MOSO-II framework is based on a multi-objective genetic algorithm, non-dominated sorting genetic algorithm II (NSGA-II) [4]. In this paper, the NSGA-II is realized through a Python-based package *pymoo* [69]. The determination of the important parameters is according to the initial settings of NSGA-II in [4] and our previous study [20]. Specifically, simulated binary crossover (SBX) and polynomial mutation (PLM) operators are defined as search parameters, with a crowding degree of 15 and 20, respectively. The probability is set as 0.9. The population size is defined as 100, while the generation size is case-specifically determined by the attainment of the convergence of the hypervolume (HV) performance indicator and the convergence of objective values. Subsequently, the termination criterion of the optimization is indicated by the generation size. In addition, since required ranges of thickness d_m can be different for different materials even when being integrated for the same applicability type, upper and lower dead bands of d_m can be individually defined for each material by using the *Repair* function in *pymoo* [69].

Overall, the workflow of the established MOSO-II framework is presented in Fig. 3 and Algorithm 1. Due to the random nature of genetic algorithms and the randomly drawn samples ξ_k in the problem (3) when using different seeds, the optimization process should be run multiple times to obtain the approximated Pareto front. In this work, the optimization process is run five times for each case.

Algorithm 1: Algorithm of MOSO-II framework

Input: Initial value of $\{\boldsymbol{x}, \boldsymbol{d}, \boldsymbol{y}\}, A, h$
Output: Pareto-optimal solutions of $\{\boldsymbol{x}, \boldsymbol{d}, \boldsymbol{y}\}$
for $i = 1 : N_{generation}$ **do**
  $u_w \leftarrow Uwall(\boldsymbol{x}, \boldsymbol{d})$;
  $u_c \leftarrow Uceiling(\boldsymbol{x}, \boldsymbol{d})$;
  $e \leftarrow NGBoost(u_w, u_c, \boldsymbol{y}, A, h)$;
  $\{\boldsymbol{x}, \boldsymbol{d}, \boldsymbol{y}\} \leftarrow NSGA2(\boldsymbol{x}, \boldsymbol{d}, \boldsymbol{y}, A, h, e)$;
end

2.7. Comparative analysis with single-stage multi-objective stochastic optimization

For a comparative study and performance validation, the proposed MOSO-II framework is compared with alternative single stage multi-objective optimization (MOSO) frameworks, as established in previous work [20]. Within the single stage MOSO frameworks, two comparative optimization problems are defined. In the first comparative optimization problem (*single-stage MOSO framework-1*), GWP and cost are optimized separately in embedded and operational forms. The optimization problem thus aims at minimizing (i) embedded GWP and (ii) investment cost of all components of passive and active strategies, as well as (iii) operational GWP and (iv) operational cost, as shown in Eq. (14):

$$\begin{aligned}
&\min_{y \in Y} \quad \sum_{i=1}^{N} G_c(k_i) + \sum_{j=1}^{J} G_{oe}(y_j) \\
&\min_{y \in Y} \quad \sum_{i=1}^{N} C_c(k_i) + \sum_{j=1}^{J} C_{oe}(y_j) \\
&\min_{y \in Y, \xi \in \mathbb{R}} \quad \mathbb{E}_P[G_o(y, u(k_i), \xi_o)] \\
&\min_{y \in Y, \xi \in \mathbb{R}} \quad \mathbb{E}_P[C_o(y, u(k_i), \xi_c, \xi_o)] \\
&s.t. \quad u(k_i) \le U
\end{aligned} \tag{14}$$

from top to bottom, the objective functions represent, in order, embedded GWP, investment cost, operational GWP and operational cost.

In the second case with *single-stage MOSO framework-2*, active and passive decisions are separately, i.e., parallelly optimized, resulting in four objectives representing the separately investigated objectives, as

Table 1
Overview of the proposed two-stage MOSO-II framework and investigated cases of using different alternative MOSO frameworks.

Framework	Equation	Description
Two-stage MOSO-II framework	(6)	Holistic consideration of passive and active design strategies as two-stage decisions
Single-stage MOSO framework-1	(14)	Separate consideration of embedded and operational values in one single stage
Single-stage MOSO framework-2	(15)	Separate consideration of passive and active design strategies in one single stage

shown in Eq. (15):

$$\begin{aligned}
&\min_{y\in Y} \quad \sum_{i=1}^{N} G_c(k_i) \\
&\min_{y\in Y} \quad \sum_{i=1}^{N} C_c(k_i) \\
&\min_{y\in Y,\xi\in\mathbb{R}} \quad \mathbb{E}_P[\sum_{j=1}^{J} G_{oe}(y_j) + G_o(y, u(k_i), \xi_o)] \\
&\min_{y\in Y,\xi\in\mathbb{R}} \quad \mathbb{E}_P[\sum_{j=1}^{J} C_{oe}(y_j) + C_o(y, u(k_i), \xi_c, \xi_o)] \\
&s.t. \quad u(k_i) \le U
\end{aligned} \tag{15}$$

from top to bottom, the objective functions represent the following in order: GWP associated with passive strategies, investment cost of passive strategies, GWP of active strategies and operational cost associated with active strategies.

The proposed MOSO-II framework and the two alternative frameworks are summarized in Table 1. Through the comparison of optimization results we can demonstrate the superiority and necessity of the established MOSO-II framework.

3. Case study

3.1. Description of the generic zone

Due to the increasing attention to large-scale sustainable building planning in districts and cities, it is important to analyze typical thermal zones within buildings as smaller units, so that the computational effort of the analysis and optimization of large-scale sustainable urban planning can be potentially reduced. Thus, as a proof of concept, a generic zone of a multi-family residential building is created, so that it can be implemented in the future optimization of large-scale urban planning. As shown in Fig. 4, the generic zone possesses one exterior façade and is adiabatic from other interior zones. The single-sided apartment has a floor area A_f of 50 m^2 and a clear floor height of 2.5 m. For effective and sufficient single-sided natural ventilation, the floor depth is defined as 2.5 times of the clear floor height, i.e., 6.25 m. In addition, for performing the life cycle impact assessment (LCIA) and life cycle cost (LCC) analysis, the reference study period is defined as 60 years representing the expected life span of the building based on [70,71].

3.2. Description of the machine learning model

To ensure a good performance of the machine learning model, we carefully process the target dataset with the steps conducted in the previous research [59]. The original domestic Energy performance certificate (EPC) dataset is filtered to exclude unnecessary uncertainties and data noise. For this purpose, building samples in the dataset are only limited to flat buildings in a mid-terrace form, built after 2014. In addition, the dataset is filtered based on the 95th percentile of all building samples regarding total operational energy consumption. Table 2 provides an overview of all filtered value range constraints.

To ensure that all information is properly recognized by the data-driven model, we use the label-encoder to pre-process all categorical features in Table 3. As for the model training process, we kept

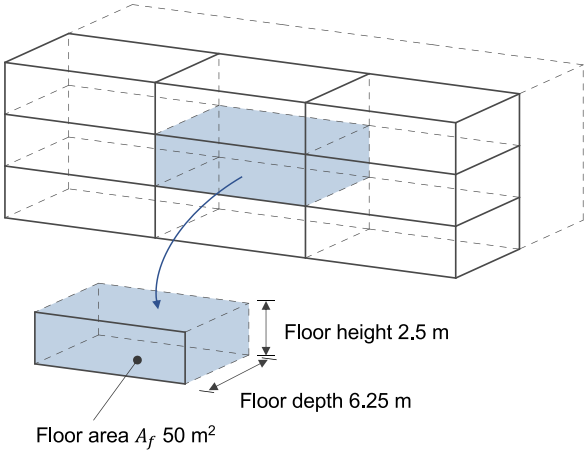

Fig. 4. Graphical illustration of the generic zone.

Table 2
Value range constraints of the features for the machine learning model.

Feature	Value range	Unit
Construction year	2014–2022	–
Building type	Flat	–
Zone position	mid-terrace	–
Floor area	29–83	m^2
Floor height	2.35–2.8	m

Table 3
Features for the machine learning model.

Feature	Unit
Floor area	m^2
Floor height	m
U-value wall	W/(m^{2}K)
U-value ceiling/floor	W/(m^{2}K)
Heat generator	- (categorical)
Heater	- (categorical)
Heating control system	- (categorical)

the model setting (NGBoost) for the scoring method (negative log-likelihood), distribution (Gaussian distribution) and base learner (Decision Tree Regressor). We fine-tuned the max depth of the base learner to 5 to ensure the best fit for the dataset. In addition, the number of estimators is defined as 1350. The dataset is split into training/test sets in 80/20 proportion, where the model is fitted in the training set and its performance is evaluated on the test set.

3.3. Passive strategy: building materials

In the case study, exterior wall and interior ceiling of the solid brick construction type are observed as passive strategies. Specifically, the double-shell construction with structural and facing bricks is investigated, as this construction type is commonly applicable in different geographical contexts, in this study in Germany and the United Kingdom. The corresponding applicability types are derived from the knowledge-based database and summarized in Tables 4 and 5 for the two building components. The material choice of individual applicability types and their corresponding thickness are included as categorical and continuous design variables. Detailed information can

Table 4
Investigated applicability types and thickness as design variables for exterior wall.

Design variable	Variable type
Facing brick	categorical
Insulated substructure (insulation)	categorical
Insulated substructure (steel)	categorical
Masonry unit	categorical
Mortar	categorical
Finish	categorical
Plaster	categorical
Thickness Brick façade	continuous
Thickness Insulated substructure (insulation)	continuous
Thickness Insulated substructure (steel)	continuous
Thickness Masonry unit	continuous
Thickness Mortar	continuous
Thickness Finish	continuous
Thickness Plaster	continuous

Table 5
Investigated applicability types and thickness as design variables for interior ceiling.

Design variable	Variable type
Flooring	categorical
Insulation hard	categorical
Screed	categorical
Reinforced concrete	categorical
Finish	categorical
plaster	categorical
Thickness Flooring	continuous
Thickness Insulation hard	continuous
Thickness Screed	continuous
Thickness Reinforced concrete	continuous
Thickness Finish	continuous
Thickness Plaster	continuous

be found in the supplementary material. As previously mentioned in 2.6, the thickness of different materials for the same applicability type can vary. The upper and lower bands of material thickness are therefore differentiated accordingly.

3.4. Active strategy: heating system

Within the scope of the case study, the investigated active design strategy is the heating system, as shown in Table 6. Accordingly, the investigated components include: heat generator, heater and heating control. Based on the dataset for training the machine learning model, five heat generators are included: air source heat pump, liquefied petroleum gas (LPG) boiler, electric boiler, mains gas boiler and ground source heat pump. As shown in Table 6, LPG tank and pipework are included as auxiliary components for LPG boiler and ground source heat pump, respectively. In addition, radiator and underfloor heating system are the investigated two heater types. As for the heating control system, five systems are included based on the dataset for training the machine learning model.

As for converting the obtained primary energy consumption to use energy consumption in the global warming potential (GWP) calculation, the system efficiency factors of the investigated heat generators according to DIN V-4701-10 [67] are applied and summarized in Table 7. By being divided by the respective system efficiency factor, the obtained primary energy consumption of different heating systems is converted to use energy.

3.5. Quantification of uncertainty parameters and scenario generation

As previously mentioned, the individual/use uncertainty is represented as the uncertain operational heating energy consumption and realized through the machine assistance approach. For this purpose, the usage of the machine learning algorithm NGBoost enables the probabilistic regression to capture the uncertainties. It means that the model learns the relationship between input and output as a distribution mapping. The range of the distribution reflects the fuzziness existing in the information carried within data that describe the target building. These are factors that affect the output but fail in being captured in the input data, or are inaccessible during the building design phase, e.g., different user behaviors, micro-climate conditions, or the actual energy efficiency of the systems. In this context, the defined Gaussian distribution reflects the distribution of operational heating energy consumption in residential buildings, which is supported by previous statistical studies described in 2.4. As NGBoost returns the distribution object with specific parameters, the probability distribution function (PDF) is known. Accordingly, the individual/use uncertainty is included in the MOSO-II framework using Eq. (3).

As for the political/market uncertainty, three scenarios of energy price inflation subject to different energy sources are generated based on the analysis of energy price development from 2008 to the first half of 2022 in Germany. As shown in Table 8, the inflation rates are determined based on the annual average price change rate compared to the previous year. While the low and high inflation rates represent the extreme cases, the moderate inflation rate is the average rate excluding the extreme inflation rates during the last 15 years. It is to mention that the prices of natural gas and electricity are based on the average consumer price of two annual consumption groups from [57], representing an annual consumption of lower than 50,000 kWh.

Through the analysis, it can be observed that the energy price of natural gas has remained relatively stable over the past 15 years despite the annual inflation, while the prices of other two energy sources have followed the usual annual inflation rate. This stability in the price of natural gas tend to explain the high dependency of Germany on natural gas over other energy sources. This also indirectly explains the shock and difficulty of many in the first half of 2022 in response to the sharp increase in natural gas prices, due to the impact of the Russia-Ukraine crisis. On the other hand, it is to mention that no steady increase in the average electricity price can be observed in the first half of 2022 in Germany. This is due to the fact that the high inflation rate in electricity price is partially mitigated by relief measures, such as elimination of the Renewable Energy Sources Act (EEG) surcharge in Germany [72]. Accordingly, the change rate indicating the high inflation scenario in the table does not stem from the first half of 2022, but from 2013. Subsequently, with the initial price of 2022 and the three scenarios of energy prices, the political/market uncertainty is included in the MOSO-II framework using Eq. (2).

4. Results

4.1. Performance of the machine learning model

The result from the machine learning model demonstrates a promising performance based on the applied assessment criteria. The coefficient of determination (R^2) reached during the validation is 0.89, which shows that about 90% of the variance of the studied dependent variable can be explained by the variance of the independent variable. The Root-Mean-Square Error (RMSE) remains at approximately 17.3. Also, since the NGBoost gives the deterministic result and a distribution, we observed a good prediction interval with 95% confidence coverage to the ground-truth values as shown in Fig. 5.

4.2. Termination criterion

As previously mentioned, the termination criterion of the investigated frameworks is case-specifically defined by the generation size, i.e., the number of iterations of the applied algorithm NSGA-II, based on the convergence of hypervolume (HV) and the convergence of objective values. Fig. 6 shows the convergence of both objective values and HV

Table 6
Design variables of heating systems in active design strategies.

Design variable	Parameter set	Global warming potential (GWP)					RSL	Investment cost
		A1-A3 [kg CO2-eq. /pcs.]	C2 [kg CO2-eq. /pcs.]	C3 [kg CO2-eq. /pcs.]	C4 [kg CO2-eq. /pcs.]	B6 [kg CO2-eq. /kWh]	[a]	[€]
Heat generator	Air source heat pump	393.00	1.54	4.35	0.03	0.17	20.00	19498.63
	Boiler (LPG)	753.50	1.29	21.82	1.58	0.25	20.00	5189.16
	Boiler (electric)	14.74	0.03	4.92	0.00	0.53	15.00	920.49
	Boiler (mains gas)	753.50	1.29	21.82	1.58	0.25	20.00	5189.16
	Ground source heat pump	393.00	1.54	4.35	0.03	0.12	20.00	19713.65
Heater	Radiator	450.23	1.02	0.08	–	–	30.00	1951.29
	Underfloor heating	256.14	0.41	221.54	–	–	30.00	1691.55
Auxiliary component	LPG tank	1720.00	5.33	0.43	–	–	18.00	1500.00
	Pipework (GSHP)	726.20	–	–	–	–	20.00	–
Heating control	Programmer and at least two room thermostats Programmer and room thermostat Programmer, room thermostat and thermostatic radiator valve (TRVs) Room tthermostat only Time and temperature zone control							

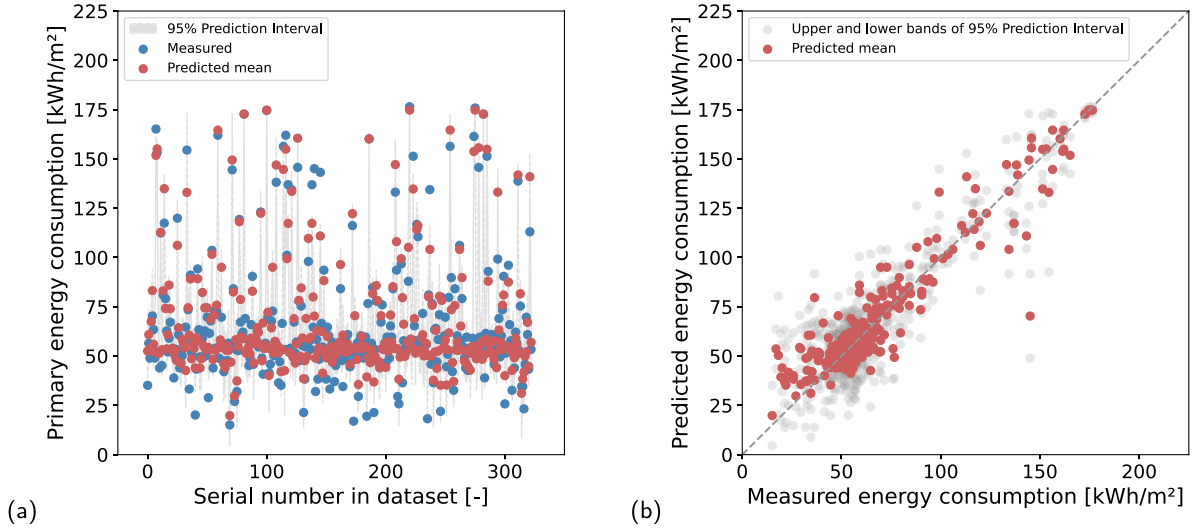

Fig. 5. Results of machine learning model: (a) relationship between measured and predicted primary energy consumption, (b) relationship between measured and predicted mean and extreme primary energy consumption.

Table 7
System efficiency factor of each boiler according to DIN V-4701-10 [67].

Heat generator	System efficiency factor
Air source heat pump	0.37
Boiler (LPG)	1.05
Boiler (electric)	1.00
Boiler (mains gas)	1.05
Ground source heat pump	0.27

value during one exemplary run of the *two-stage MOSO-II framework*, which is subject to the constraints of thermal transmittance (U-values) imposed by Nearly Zero Energy Building (NZEB) and German Building Energy Act (GEG), respectively. The optimization process is well illustrated in the figure: starting from a population size of 100, the population size increased in steps of 100 during the iteration. It can be observed in Fig. 6(a) that the objective values decline substantially during the first 15,000 function evaluations, i.e., 150 generations, and gradually stabilizes by the 200th generation. Similarly, in Fig. 6(b), a significant increase can be seen during the first 150 generations, followed by a gradual stabilization starting from the 200th generation. Based on the convergence results and to ensure a certain degree of fault tolerance when generating random numbers with different seeds, the termination criterion of the applied algorithm within the *two-stage MOSO-II framework* is determined as 300 iterations, i.e., a generation size of 300. In a comparable way, the termination criteria of the other two cases with different single-stage MOSO frameworks are also defined.

4.3. Optimization results

With the proposed *two-stage MOSO-II framework*, multiple iterations yield approximated Pareto fronts for the studied case described in 3. The obtained Pareto fronts are constrained by GEG and NZEB requirements, respectively. In general, when compared to alternative single-stage MOSO frameworks, the *two-stage MOSO-II framework* delivers a smaller number of Pareto-optimal solutions and is more compact. Specifically, while the number of Pareto-optimal points from single-stage MOSO frameworks is always 100, which corresponds to the population size, the average number of Pareto-optimal points from the two-stage MOSO-II framework is 10 when constrained by NZEB and 18 when constrained by GEG. Since the targeted objectives are different in the frameworks, it is hard to intuitively compare the Pareto fronts. For example, as shown in Eq. (14) and Eq. (15), the two single-stage MOSO frameworks each have four objectives, which is not easy to

Table 8
Scenarios of energy price with different energy sources based on analysis of the development of energy prices from [56,57].

	Price 2022	Low inflation		Moderate inflation		High inflation	
	[€/kWh]	Change rate	Probability	Change rate	Probability	Change rate	Probability
Electricity	0.314	−2.19%	6.67%	2.76%	86.67%	10.90%	6.67%
Liquefied Petroleum Gas	0.137	−18.06%	6.67%	3.03%	86.67%	30.67%	6.67%
Natural gas	0.097	−7.22%	13.33%	−0.20%	80.00%	25.85%	6.67%

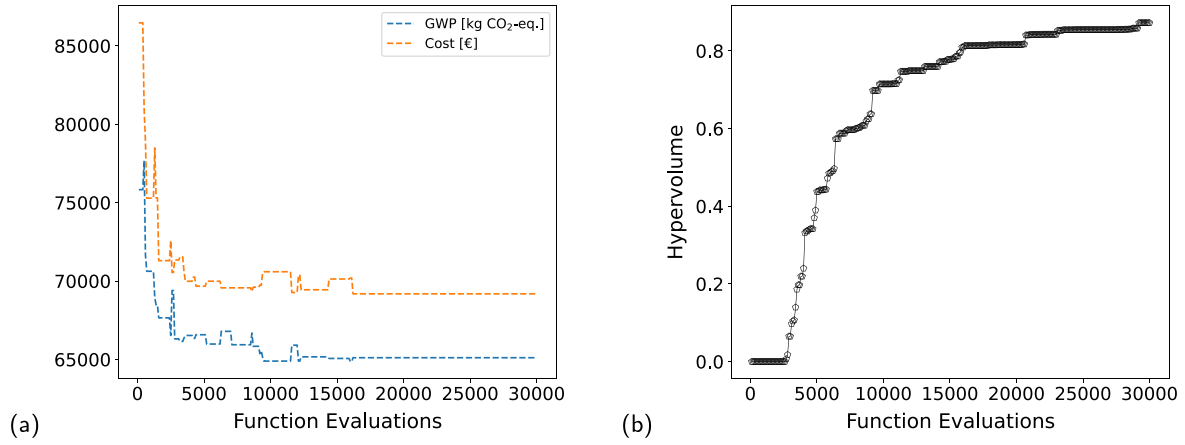

Fig. 6. Results of convergence during one exemplary run of the MOSO-II framework: (a) convergence of objective values of the case constrained by NZEB, (b) convergence of hypervolume (HV) of the case constrained by GEG.

visualize. Thus, in order to provide an initial assessment of the performance of the frameworks and to examine the optimized results of all stages, regardless of how the objectives were initially formulated, the cumulative costs and global warming potential (GWP) were aggregated, respectively. In this way, the four-dimensional optimization results of the single-stage MOSO frameworks are illustrated in a two-dimensional manner and the cumulative GWP and cost from all decision stages can be obtained. Fig. 7 demonstrates the comparison when subjected to the constraint of the GEG requirement. It is to note that the blue points for both single-stage MOSO frameworks are the obtained Pareto-optimal points from all iterations that are illustrated in a two-dimensional way. For instance, in 7(a), the optimization results of embedded and operational GWP are aggregated and the optimization results of investment and operational cost are aggregated. It can be observed that the results from the *two-stage MOSO-II framework* outperform those of the other two single-stage MOSO frameworks by being closer to the origin, indicating lower objective values. Moreover, it can be seen that the results of the *single-stage MOSO framework-1* exhibit a larger span compared to the other two frameworks. Similar results can also be observed when constrained by the NZEB requirement. As a result, it is evident that a holistic consideration of passive and active design strategies as two-stage decisions leads to a lower objective value of the total GWP and cost within a more confined range.

When analyzing the derived passive and active optimal solutions, statistical analysis is performed (see the "Top ten common variable combination through investigated frameworks" in the supplementary material). It can be observed that certain design variables remain relatively unaffected by different frameworks and remains consistent. For example, underfloor heating is observed as the optimal heater type over radiators in almost all design solution sets. Regarding the obtained optimal heat generator, mains gas boiler is the sole solution for both the *two-stage MOSO-II framework* and *single-stage MOSO framework-2* under both GEG and NZEB constraints, while the electricity-driven boiler emerges as the most prevalent option derived from *single-stage MOSO framework-1*.

On the other hand, some design variables exhibit considerable diversity. The most varying variables include insulated substructure (insulation), masonry unit, flooring, insulation hard and heating control system. Figs. 8–10 exemplarily show the statistical overview of the obtained Pareto-optimal design solutions of insulated substructure (insulation), masonry unit and heating control system, constrained by the NZEB requirement. Overall, in the *two-stage MOSO-II framework*, it is evident that there is a decrease in the total count of optimal solutions, as well as a notable difference in the most frequently occurring solutions compared to those derived from the other two frameworks. As Fig. 8 demonstrates, rock wool insulation in low density range and flax fleece are the two most commonly appearing optimal solutions for exterior wall insulation. However, while the prevalence of rock wool insulation in low density range remains dominant in both single-stage MOSO frameworks, flax fleece is the most frequently appearing option obtained from the *two-stage MOSO-II framework*. Comparably, despite the general dominance of concrete masonry bricks in all Pareto-optimal solution sets, lightweight concrete block from 100% natural pumice is leading regarding the frequency of occurrence in the *two-stage MOSO-II framework*. As for the two alternative frameworks, lightweight masonry blocks from natural aggregates (solid brick light) is the most prevalent option (see Fig. 9). As for active strategies, the heating control system is the most varying variable, where "time and temperature zone control" and "room thermostat only" are the two dominating options.

Similarly, the continuous variables representing material thickness demonstrate variability in certain cases while remaining constant in others. Among all, the insulation of insulated substructure and masonry unit of exterior wall have the most varying thickness due to their predominant contribution to the U-value of the exterior wall. Table 9 and Fig. 11 show the comparison of the obtained thicknesses of the aforementioned two applicability types within different frameworks. Overall, it can be observed that the thickness range of the materials is reduced within the *two-stage MOSO-II framework*, while the mean value does not significantly vary. It indicates a better performance of the proposed *two-stage MOSO-II framework* in also narrowing down the range of continuous variables. In addition, generally greater thickness can be seen in exterior wall insulation when constrained by the NZEB requirement, which reveals the influence of a higher standard of U-value on the results and proves the plausibility of the obtained results.

4.4. Performance validation of pareto-optimal design solutions

Since the objectives' expected values (EV) are optimized through stochastic programming, the actual GWP and cost subjected to the

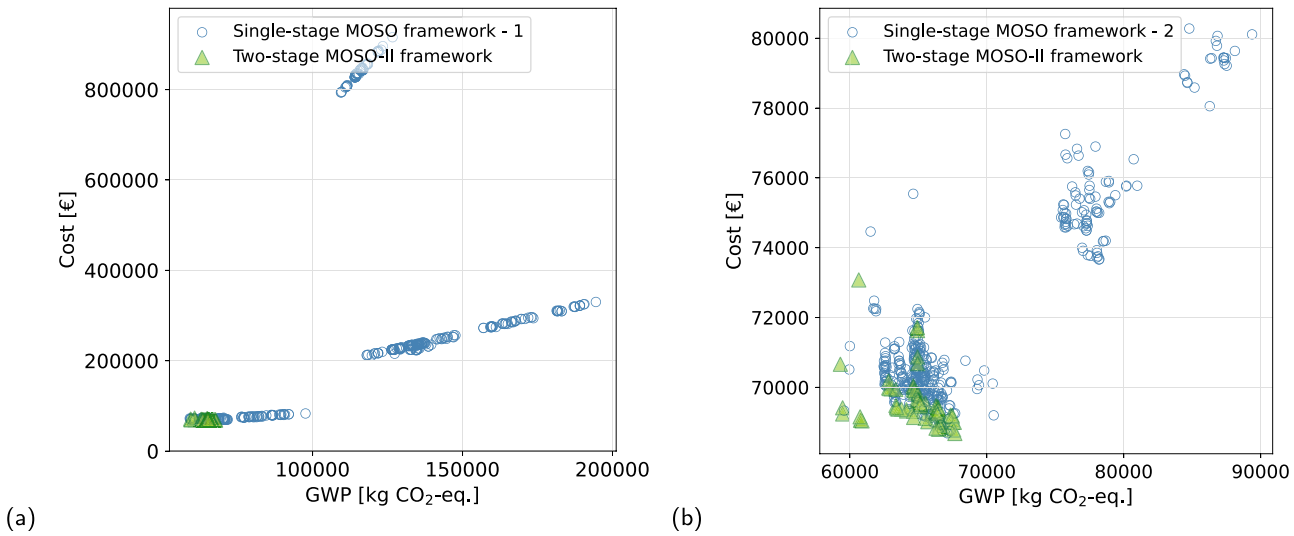

Fig. 7. The total GWP and cost of all decision stages based on all the obtained optimal expected values (EV) of the two-stage MOSO-II framework, constrained by the GEG requirement, compared with: (a) single-stage MOSO framework-1, (b) single-stage MOSO framework-2.

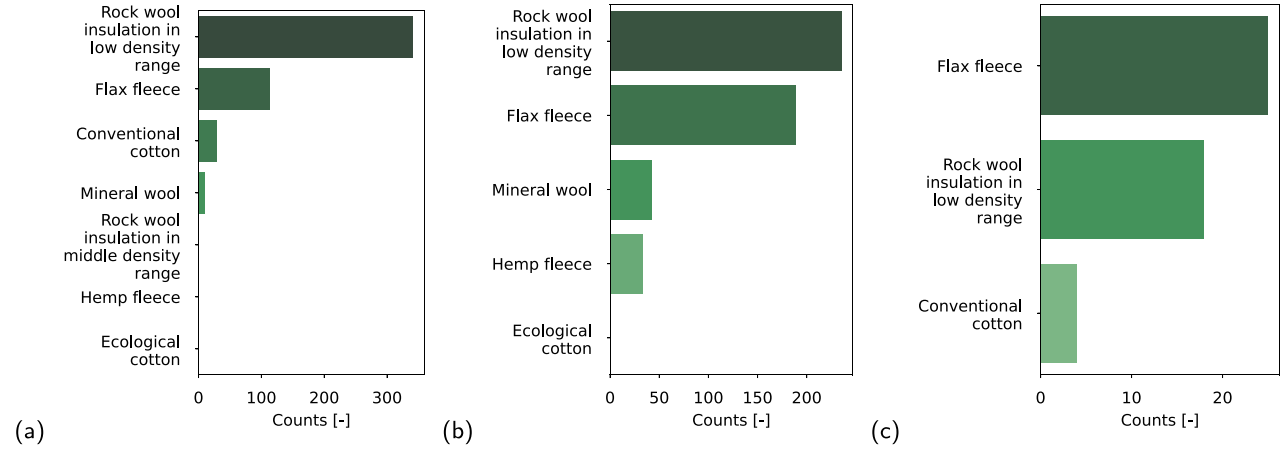

Fig. 8. Statistical overview of Pareto-optimal design solutions of insulated substructure (insulation), constrained by the NZEB requirement, from: (a) single-stage MOSO framework-1, (b) single-stage MOSO framework-2, (c) two-stage MOSO-II framework.

ultimately realized uncertainty parameters can be higher or lower than the obtained objective values. Thus, to further validate the performance of the proposed *two-stage MOSO-II framework*, a Monte Carlo approach is applied to present different outcomes under various uncertainty parameters. By randomly drawing samples of uncertainty parameters 50 times, performance validation results of the Pareto-optimal design solutions are obtained.

Fig. 12 shows the comparison of the performance validation results of Pareto-optimal design solutions from different frameworks, focusing specifically on GWP. Herein, results under different energy standard constraints are also distinguished. As Fig. 12(a) shows, the mean GWP of passive strategies is higher for the *two-stage MOSO-II framework* than the other single-stage MOSO frameworks. In addition, the larger span of the Pareto front exhibited by the *single-stage MOSO framework-1* is also evident in the performance validation. Similar findings can be more evidently observed in the total GWP embedded in both building materials and heating, ventilation and air-conditioning (HVAC) components, as shown in Fig. 12(b). Despite the higher GWP embedded in building materials and HVAC components, Fig. 12(c) exhibits that the Pareto-optimal solutions derived from the *two-stage MOSO-II framework* result in a lower and smaller range of total GWP over the reference study period of 60 years. Accordingly, the performance of the proposed *two-stage MOSO-II framework* is further validated by the capability of efficiently minimizing the total GWP. Moreover, as shown in Fig. 12(d), throughout the reference period, the embedded GWP derived from the *two-stage MOSO-II framework* takes up a higher ratio on average. This observation can be explained by a greater material amount required to achieve a lower U-value, which leads to a reduction in the operational heating energy consumption and consequently leads to a decrease in the total GWP over the reference study period. It further reveals the importance of implementing appropriate passive design strategies.

As for the validation regarding cost, in addition to the individual/use uncertainty, the political/market uncertainty has also been considered by implementing the three inflation scenarios. Fig. 13 illustrates the performance results of the obtained Pareto-optimal design solutions. Herein, the resulted total cost throughout the reference study period and the corresponding share of investment cost within the total cost are shown. It is evident that the *single-stage MOSO framework-1* exhibits a wider range of results and the *two-stage MOSO-II framework* demonstrates its superior performance also in terms of cost. Furthermore, it is important to mention that the likelihood of scenarios with consecutively low or high inflation occurring throughout the entire reference study period of 60 years could be extremely low. The result comparison presented here primarily serves as a demonstration of the impact of different realized uncertainty parameters rather than a realistic depiction of consecutive inflation scenarios.

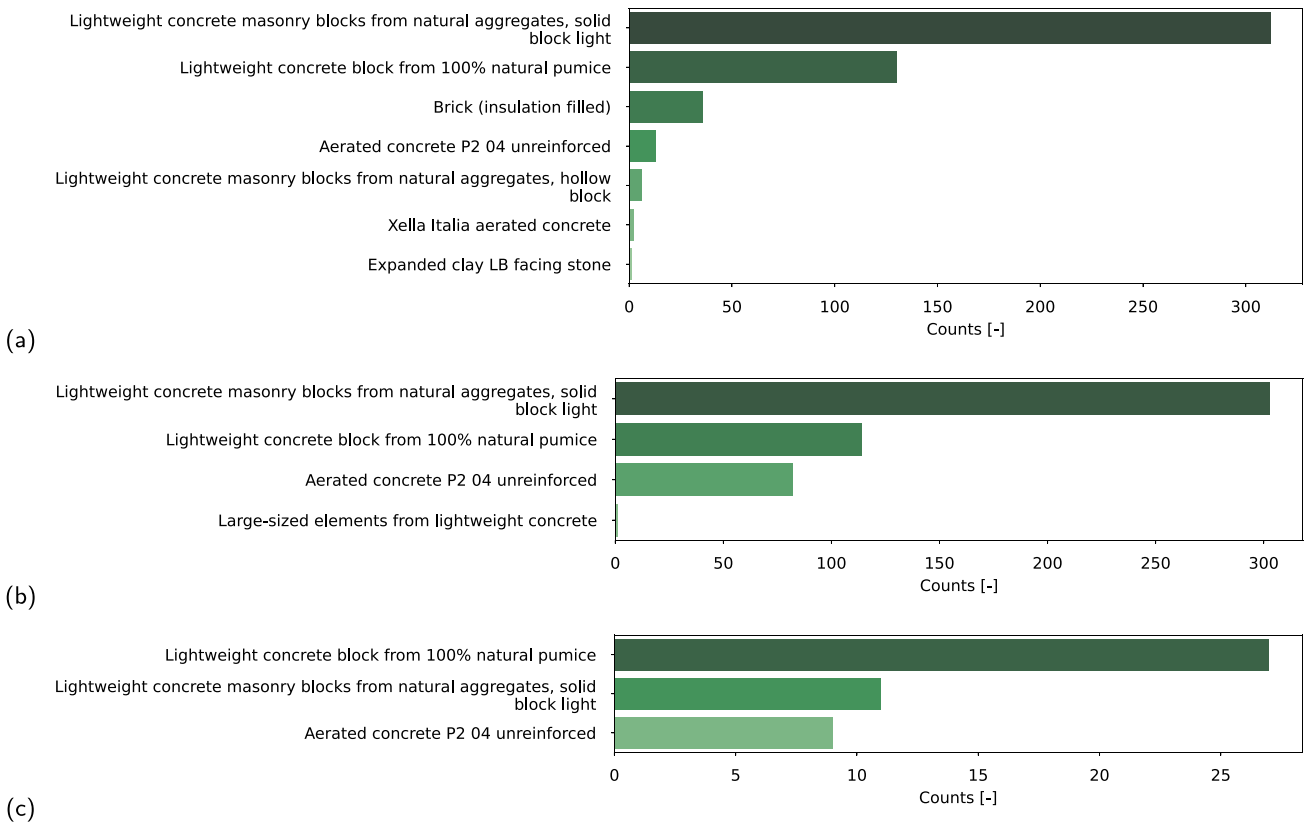

Fig. 9. Statistical overview of Pareto-optimal design solutions of masonry unit, constrained by the NZEB requirement, from: (a) single-stage MOSO framework-1, (b) single-stage MOSO framework-2, (c) two-stage MOSO-II framework.

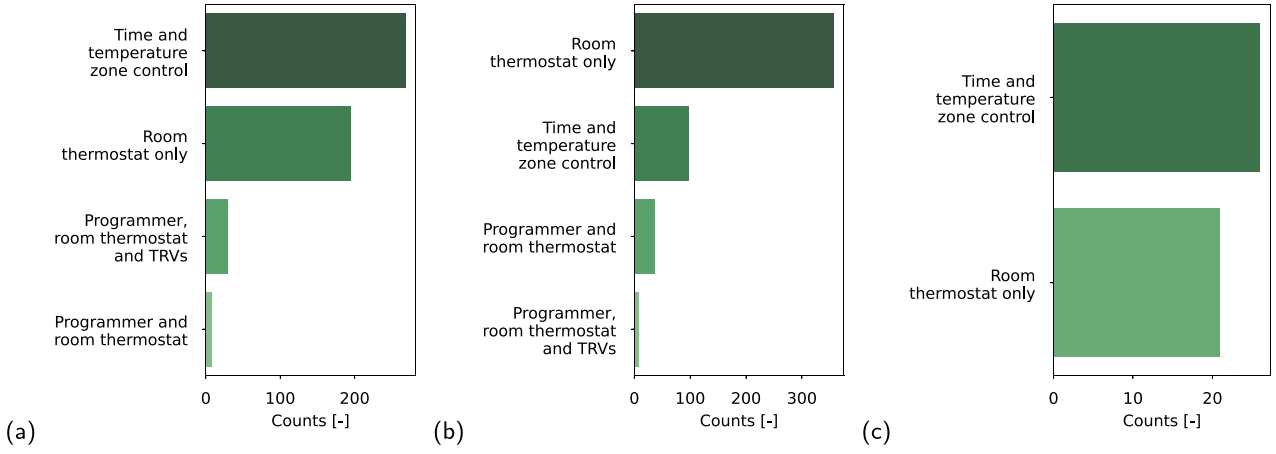

Fig. 10. Statistical overview of Pareto-optimal design solutions of heating control system, constrained by the NZEB requirement, from: (a) single-stage MOSO framework-1, (b) single-stage MOSO framework-2, (c) two-stage MOSO-II framework.

5. Discussion

In the building sector, decisions towards sustainable building planning can be divided into passive and active strategies, which are usually made at different points in time. Despite the increasing number of studies focusing on finding optimal solutions considering trade-offs, only limited studies expand the scope of exploration towards different decision stages in the building industry [38,39]. Thus, this paper presents a holistic multi-objective stochastic decision-making framework, the *two-stage MOSO-II framework*, in which passive and active design strategies are segmented into two decision stages and uncertainty is considered. Aiming at minimizing total global warming potential (GWP) throughout the entire building cycle and life cycle cost (LCC) analysis, the proposed framework included two decision stages: first-stage decisions refer to the passive design strategies and second-stage decisions refer to active design strategies. Compared to [38], the proposed approach defines optimization stages that reflect the real-world decision stages instead of stages of conducting decision-making approaches or frameworks.

Moreover, different from [39], the proposed framework takes uncertainty in the decision-making process into account. Based on the

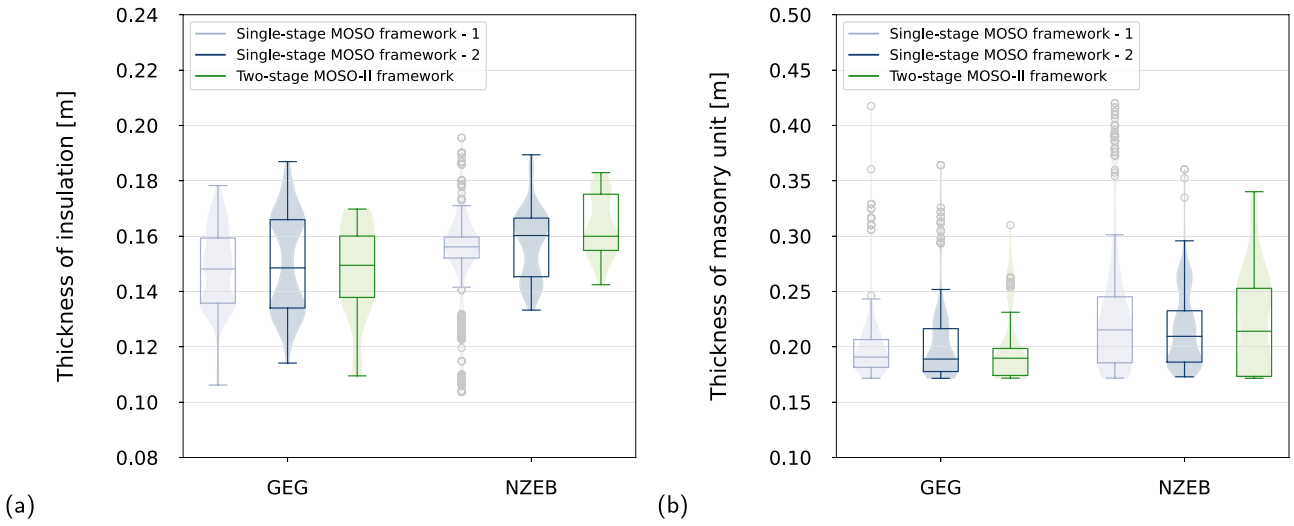

Fig. 11. Comparison of material thicknesses of selected applicability types: (a) insulated substructure (insulation), (b) masonry unit.

Table 9
Results of the material thicknesses of selected applicability types.

Applicability type	Framework	GEG (U-value with 0.21 W/m^{2}K)		NZEB (U-value with 0.18 W/m^{2}K)	
		Thickness range [m]	Mean thickness [m]	Thickness range [m]	Mean thickness [m]
Insulated substructure (insulation)	Single-stage MOSO framework-1	0.11–0.18	0.15	0.10–0.20	0.15
	Single-stage MOSO framework-2	0.11–0.19	0.15	0.13–0.19	0.16
	Two-stage MOSO-II framework	0.11–0.17	0.15	0.14–0.18	0.16
Masonry unit	Single-stage MOSO framework-1	0.17–0.42	0.20	0.17–0.42	0.23
	Single-stage MOSO framework-2	0.17–0.36	0.20	0.17–0.36	0.22
	Two-stage MOSO-II framework	0.17–0.31	0.20	0.17–0.34	0.22

classification principle from previous work [20], two types of uncertainty are considered in this study: individual/use uncertainty and political/market uncertainty. The two types of uncertainty cover both the uncertainty related to individual objects and global dynamics and thus enrich the uncertainty catalogue of the previous work.

Through a case study of a generic zone with solid brick construction and a heating system, the proposed *two-stage MOSO-II framework* is examined and compared with alternative single-stage MOSO frameworks. Through the optimization process, a set of Pareto-optimal solutions can be generated and serves as an optimal decision catalogue for planners and decision-makers. Results show that the *two-stage MOSO-II* framework outperforms the other two alternative frameworks in terms of obtaining lower objective values and narrowing down the potential solutions further to a smaller range in both categorical and continuous variables. Accordingly, a better decision catalogue with a smaller range of optimal solutions can be provided. This leads to a reduced effort in choosing the proper design strategies in the early phase of building planning. In contrast to conventional approaches of providing all possible solutions in early design phases, as in [26,27], the methodology proposed in this study is able to exclude irrelevant information regarding poorly performing design solutions to the fullest extent possible so that decision-making in early design stages can be possibly easier. After obtaining the optimal solutions, multi-criteria decision-making (MCDM) strategies, as shown in the previous study [20], can be additionally applied to rank the derived passive and active solutions. Depending on the preference of different stakeholders, the weighting factor of different criteria can be different, which can influence the ranking of the optimal solutions. Subsequently, after choosing the proper design solutions, a more reliable life cycle impact assessment (LCIA) calculation can be conducted during the early modeling process with software, such as building information modeling (BIM).

Meanwhile, some insights can be provided by the obtained Pareto-optimal solutions. For active design strategies, the heating control system is the most varying variable, while most variables of active design strategies have no significant change. According to the results of this paper, mains gas boiler and floor heating are almost the sole optimal solution for heat generator and heater, respectively. This choice of heat generator is based on previous market conditions and reflects the high dependency on natural gas in Germany in the past two decades. It can be explained by the relatively insignificant disadvantage of natural gas regarding GWP and its significant price advantage in terms of low unit price and stability in price change. Hence, to reduce the dependency on imported natural gas, it is important to adjust the energy price of natural gas. On the other hand, to promote electricity as the optimal solution for future heating source, it is important to increase the ratio of renewable energy source in the electricity mix to further expand its advantage in GWP. As for passive design strategies, it is to observe that the most varying categorical design variables are insulated substructure (insulation), masonry unit, flooring and insulation hard. Comparably, the most varying continuous variables are the thickness of insulated substructure (insulation) and masonry unit for exterior wall. This reflects their predominant contribution to the U-value of the exterior wall and, subsequently, to the operational energy consumption. Overall, the importance of the investigated passive design strategies can be revealed. In addition, through the performance validation of the obtained Pareto-optimal solutions, it is to observe that a lower U-value achieved by a larger amount of materials, which leads to higher embedded GWP, can affect the operational energy consumption and thus result in a reduction in the overall GWP over the whole life cycle. This finding further emphasizes the importance of the passive strategies in the decision-making process of sustainable building design.

Nevertheless, to explore the topic further, certain aspects of the presented study should be expanded further. First, in this study, passive

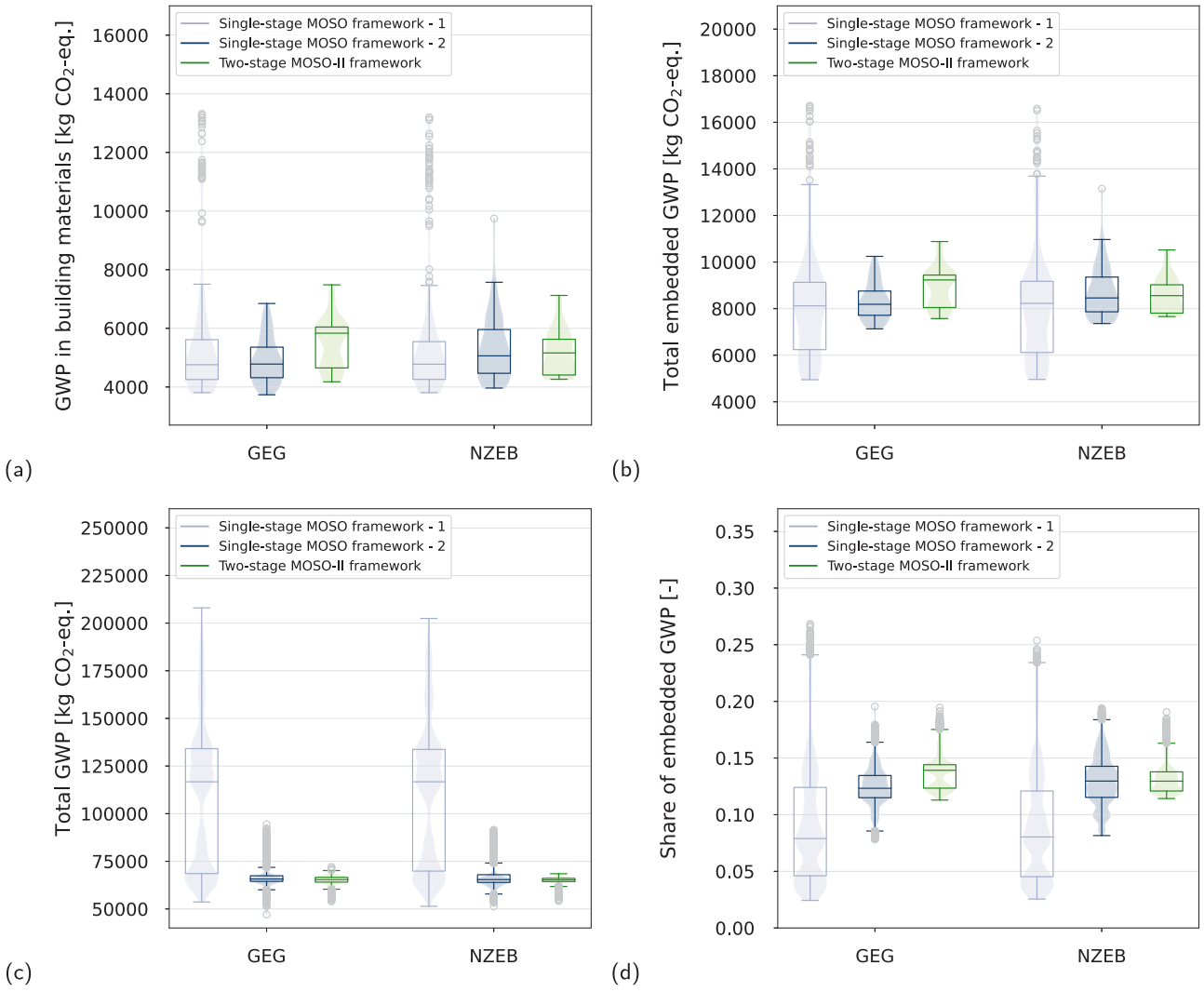

Fig. 12. Performance validation of the obtained Pareto-optimal design solutions from different frameworks in detailed analysis: (a) embedded GWP in building materials, (b) total embedded GWP of both passive and active strategies, (c) total GWP over the reference study period, (d) percentage share of total embedded GWP over total GWP.

and active design strategies are represented by the material choice of selected building components and heating systems, respectively. A further investigation on other design strategies is required. For example, passive strategies include thermal mass, building orientation, structure, building geometry, window-to-wall ratio, solar protection, etc. Accordingly, it is worth implementing the proposed approach in diverse building contexts with more than one zone and investigating various variables of building geometry and form. In this way, a more complicated decision-making process can potentially be supported. On the other hand, active strategies include mechanical ventilation, cooling and using thermal collectors and photovoltaic. In this context, optimal solutions of cooling systems and synergistic effects between cooling and heating demand are increasingly interesting due to the rising cooling demand. The uncertainty catalogue should also be further expanded to include more uncertainty parameters and define them in a more profound way. For example, the uncertain energy efficiency of systems can be modeled in more detail. And regarding the definition of the decision stages and objectives, the proposed framework can also be further investigated and potentially expanded. For instance, it can be interesting to integrate heating load as an intermediate design variable or a separate objective in the optimization framework. Similarly, other design decisions and objectives can also be investigated to improve the fineness of the proposed framework. Furthermore, due to the geographical restriction of the employed dataset for training the machine learning model and the fact that the database covering ecological and economical information is mainly based on German context, the case study exclusively investigates the double-shell brick construction, and this might influence the reliability of the obtained results. Thus, it is of interest to validate the framework with other datasets and implement the proposed framework in other economic markets and geographical contexts to further expand the applicability. In addition, a generic zone is investigated in the case study to test the applicability of the proposed methodology. In future work, it should be further investigated how different generic zone types can be used to optimize design decisions on a larger scale, e.g., in urban planning. In this way, buildings with different geometries and characteristics can be potentially abstracted into different zone types to simplify the optimization process. Also, we encourage researchers to validate the proposed framework on a building scale to validate its performance.

At last, a great number of studies have investigated the influence of dynamic change in the economic context on the decision-making process, while only limited studies touched the dynamic development of environmental impacts of building products in the context of decision-making, e.g., dynamic GWP of building materials according to varying energy mix structure. It is especially important for assisting the

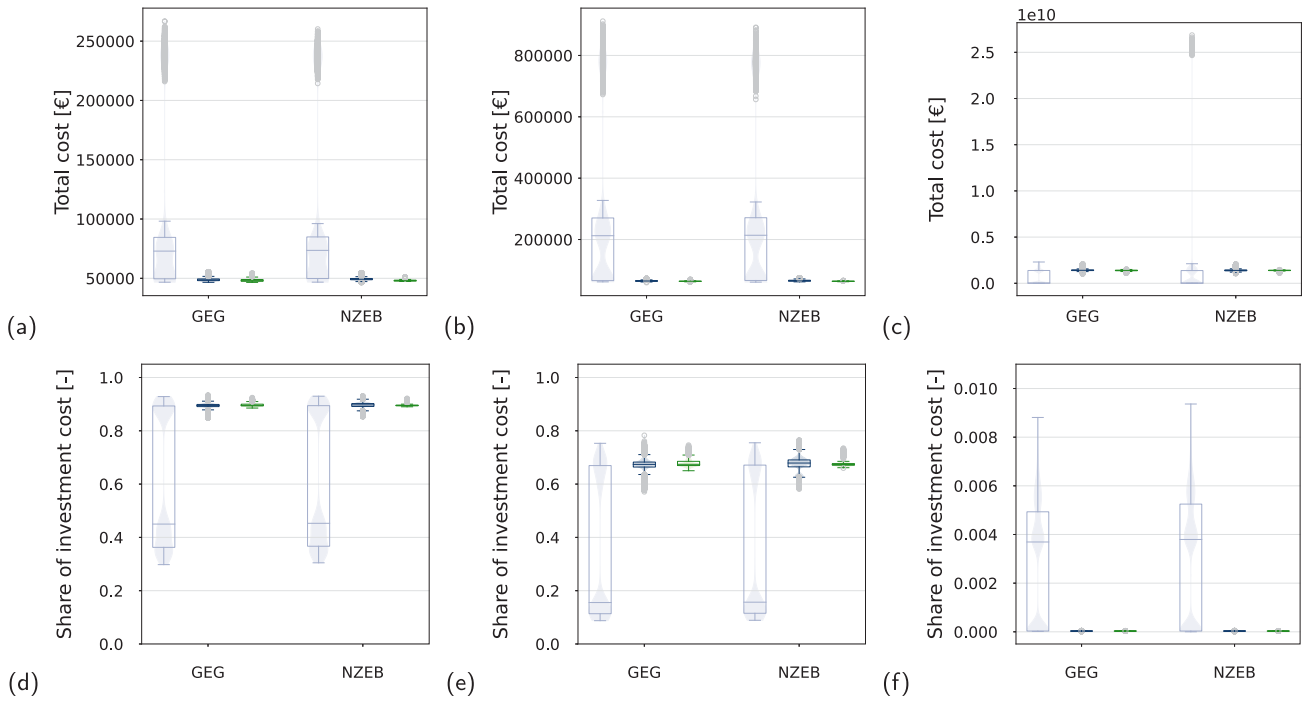

Fig. 13. Performance validation of the obtained Pareto-optimal design solutions from different frameworks in detailed analysis: (a) total cost with low inflation, (b) total cost with moderate inflation, (c) total cost with high inflation, (d) share of investment cost with low inflation, (e) share of investment cost with moderate inflation, (f) share of investment cost with high inflation.

decision-making process of municipalities and on a national level. Accordingly, in a longer view, it is important to consider the dynamic development of both aspects of GWP, i.e., dynamic life cycle assessment (DLCA), and economics to perform a more equivalent comparison and optimization, which is our next research focus.

6. Conclusion

This paper presents a *two-stage multi-objective stochastic optimization MOSO-II framework* by dividing decisions on passive and active design strategies in two stages in succession to reflect the real-world decision-making process. Furthermore, individual/use and political/market uncertainties are considered prior to decisions being made to ensure the robustness of the obtained solutions. Through a case study of a generic zone in a solid brick construction and a heating system, the advantages of the proposed *two-stage MOSO-II framework* are validated through a comparison with alternative single-stage MOSO frameworks in terms of achieving lower global warming potential (GWP) and cost throughout the entire life cycle of a building and narrowing down the optimal solutions to a small range. In addition, the results emphasize the importance of passive design strategies in sustainable building planning. The future energy mix structure and cost of energy sources should be carefully adjusted to promote a more ecologically sustainable building design.

CRediT authorship contribution statement

Chujun Zong: Writing – review & editing, Writing – original draft, Methodology, Formal analysis, Data curation, Conceptualization. **Xia Chen:** Writing – review & editing, Resources, Data curation. **Fatma Deghim:** Writing – review & editing, Data curation. **Johannes Staudt:** Writing – review & editing, Project administration, Data curation. **Philipp Geyer:** Writing – review & editing, Resources. **Werner Lang:** Writing – review & editing, Supervision, Resources, Funding acquisition.

Declaration of competing interest

The authors declare that they have no known competing financial interests or personal relationships that could have appeared to influence the work reported in this paper.

Data availability

Data will be made available on request.

Acknowledgments

This research was funded by the Deutsche Forschungsgemeinschaft (German Research Foundation, DFG) under grant FOR2363—project number: 271444440. The authors thank the reviewers for their valuable suggestions which helped to improve the quality of this paper.

Appendix A. Supplementary data

Supplementary material related to this article can be found online at https://doi.org/10.1016/j.buildenv.2024.111211.

References

[1] A. Borrmann, M. König, C. Koch, J. Beetz, Building Information Modeling: Why? What? How?, Springer, 2018.
[2] M. Manni, A. Nicolini, Multi-objective optimization models to design a responsive built environment: A synthetic review, Energies 15 (2) (2022) 486.
[3] P. Chastas, T. Theodosiou, D. Bikas, Embodied energy in residential buildings-towards the nearly zero energy building: A literature review, Build. Environ. 105 (2016) 267–282.
[4] K. Deb, A. Pratap, S. Agarwal, T. Meyarivan, A fast and elitist multiobjective genetic algorithm: NSGA-II, IEEE Trans. Evol. Comput. 6 (2) (2002) 182–197.
[5] R. Azari, S. Garshasbi, P. Amini, H. Rashed-Ali, Y. Mohammadi, Multi-objective optimization of building envelope design for life cycle environmental performance, Energy Build. 126 (2016) 524–534.
[6] N. Abdou, Y.E. Mghouchi, S. Hamdaoui, N.E. Asri, M. Mouqallid, Multi-objective optimization of passive energy efficiency measures for net-zero energy building in Morocco, Build. Environ. 204 (2021) 108141.

[7] A. Ciardiello, F. Rosso, J. Dell'Olmo, V. Ciancio, M. Ferrero, F. Salata, Multi-objective approach to the optimization of shape and envelope in building energy design, Appl. Energy 280 (2020) 115984.

[8] R. Gagnon, L. Gosselin, S.A. Decker, Performance of a sequential versus holistic building design approach using multi-objective optimization, J. Build. Eng. 26 (2019) 100883.

[9] S. Chang, D. Castro-Lacouture, Y. Yamagata, Decision support for retrofitting building envelopes using multi-objective optimization under uncertainties, J. Build. Eng. 32 (2020) 101413.

[10] Z. Fan, M. Liu, S. Tang, A multi-objective optimization design method for gymnasium facade shading ratio integrating energy load and daylight comfort, Build. Environ. 207 (2022) 108527.

[11] F. De Luca, A. Sepúlveda, T. Varjas, Multi-performance optimization of static shading devices for glare, daylight, view and energy consideration, Build. Environ. 217 (2022) 109110.

[12] S. Yeom, J. An, T. Hong, S. Kim, Determining the optimal visible light transmittance of semi-transparent photovoltaic considering energy performance and occupants' satisfaction, Build. Environ. (2023) 110042.

[13] L. Gabrielli, A.G. Ruggeri, Developing a model for energy retrofit in large building portfolios: Energy assessment, optimization and uncertainty, Energy Build. 202 (2019) 109356.

[14] H. Harter, M.M. Singh, P. Schneider-Marin, W. Lang, P. Geyer, Uncertainty analysis of life cycle energy assessment in early stages of design, Energy Build. 208 (2020) 109635.

[15] M.M. Singh, P. Geyer, Information requirements for multi-level-of-development BIM using sensitivity analysis for energy performance, Adv. Eng. Inform. 43 (2020) 101026.

[16] C.J. Hopfe, J.L. Hensen, Uncertainty analysis in building performance simulation for design support, Energy Build. 43 (10) (2011) 2798–2805.

[17] W. Belazi, S.-E. Ouldboukhitine, A. Chateauneuf, A. Bouchair, Uncertainty analysis of occupant behavior and building envelope materials in office building performance simulation, J. Build. Eng. 19 (2018) 434–448.

[18] Z. Liu, X. Zhou, W. Tian, X. Liu, D. Yan, Impacts of uncertainty in building envelope thermal transmittance on heating/cooling demand in the urban context, Energy Build. 273 (2022) 112363.

[19] A. Kamari, B.M. Kotula, C.P.L. Schultz, A BIM-based LCA tool for sustainable building design during the early design stage, Smart Sustain. Built Environ. (2022).

[20] C. Zong, M. Margesin, J. Staudt, F. Deghim, W. Lang, Decision-making under uncertainty in the early phase of building façade design based on multi-objective stochastic optimization, Build. Environ. 226 (2022) 109729.

[21] H. Li, Y. Li, Z. Wang, S. Shao, G. Deng, H. Xue, Z. Xu, Y. Yang, Integrated building envelope performance evaluation method towards nearly zero energy buildings based on operation data, Energy Build. 268 (2022) 112219.

[22] M. Koniorczyk, W. Grymin, M. Zygmunt, D. Bednarska, A. Wieczorek, D. Gawin, Stochastic energy-demand analyses with random input parameters for the single-family house, in: Building Simulation, Vol. 15, No. 3, 2022, pp. 357–371.

[23] J. Mukkavaara, F. Shadram, An integrated optimization and sensitivity analysis approach to support the life cycle energy trade-off in building design, Energy Build. 253 (2021) 111529.

[24] A. Hollberg, G. Genova, G. Habert, Evaluation of BIM-based LCA results for building design, Autom. Constr. 109 (2020) 102972.

[25] P. Tecchio, J. Gregory, R. Ghattas, R. Kirchain, Structured under-specification of life cycle impact assessment data for building assemblies, J. Ind. Ecol. 23 (2) (2019) 319–334.

[26] J. Hester, T.R. Miller, J. Gregory, R. Kirchain, Actionable insights with less data: guiding early building design decisions with streamlined probabilistic life cycle assessment, Int. J. Life Cycle Assess. 23 (2018) 1903–1915.

[27] P. Schneider-Marin, T. Stocker, O. Abele, M. Margesin, J. Staudt, J. Abualdenien, W. Lang, EarlyData knowledge base for material decisions in building design, Adv. Eng. Inform. 54 (2022) 101769.

[28] J. Hester, J. Gregory, F.-J. Ulm, R. Kirchain, Building design-space exploration through quasi-optimization of life cycle impacts and costs, Build. Environ. 144 (2018) 34–44.

[29] A. Galimshina, M. Moustapha, A. Hollberg, P. Padey, S. Lasvaux, B. Sudret, G. Habert, What is the optimal robust environmental and cost-effective solution for building renovation? Not the usual one, Energy Build. 251 (2021) 111329.

[30] Z. Liu, L. Li, S. Wang, X. Wang, Optimal design of low-carbon energy systems towards sustainable cities under climate change scenarios, J. Clean. Prod. 366 (2022) 132933.

[31] Z. Liu, Y. Cui, J. Wang, C. Yue, Y.S. Agbodjan, Y. Yang, Multi-objective optimization of multi-energy complementary integrated energy systems considering load prediction and renewable energy production uncertainties, Energy 254 (2022) 124399.

[32] S.B. Sadineni, S. Madala, R.F. Boehm, Passive building energy savings: A review of building envelope components, Renew. Sustain. Energy Rev. 15 (8) (2011) 3617–3631.

[33] R. Zhang, Y. Nie, K.P. Lam, L.T. Biegler, Dynamic optimization based integrated operation strategy design for passive cooling ventilation and active building air conditioning, Energy Build. 85 (2014) 126–135.

[34] X. Sun, Z. Gou, S.S.-Y. Lau, Cost-effectiveness of active and passive design strategies for existing building retrofits in tropical climate: Case study of a zero energy building, J. Clean. Prod. 183 (2018) 35–45.

[35] A. de Gracia, L. Navarro, J. Coma, S. Serrano, J. Romaní, G. Pérez, L.F. Cabeza, Experimental set-up for testing active and passive systems for energy savings in buildings–lessons learnt, Renew. Sustain. Energy Rev. 82 (2018) 1014–1026.

[36] A. Hajare, E. Elwakil, Integration of life cycle cost analysis and energy simulation for building energy-efficient strategies assessment, Sustainable Cities Soc. 61 (2020) 102293.

[37] J. Xu, J.-H. Kim, H. Hong, J. Koo, A systematic approach for energy efficient building design factors optimization, Energy Build. 89 (2015) 87–96.

[38] M. Hamdy, A. Hasan, K. Siren, A multi-stage optimization method for cost-optimal and nearly-zero-energy building solutions in line with the EPBD-recast 2010, Energy Build. 56 (2013) 189–203.

[39] Y. Xu, G. Zhang, C. Yan, G. Wang, Y. Jiang, K. Zhao, A two-stage multi-objective optimization method for envelope and energy generation systems of primary and secondary school teaching buildings in China, Build. Environ. 204 (2021) 108142.

[40] G. Mavromatidis, K. Orehounig, J. Carmeliet, Design of distributed energy systems under uncertainty: A two-stage stochastic programming approach, Appl. Energy 222 (2018) 932–950.

[41] F. Bagheri, H. Dagdougui, M. Gendreau, Stochastic optimization and scenario generation for peak load shaving in Smart District microgrid: sizing and operation, Energy Build. 275 (2022) 112426.

[42] J. Staudt, M. Margesin, C. Zong, F. Deghim, W. Lang, A. Zahedi, F. Petzold, P. Schneider-Marin, Life cycle potentials and improvement opportunities as guidance for early-stage design decisions, in: ECPPM 2022-EWork and EBusiness in Architecture, Engineering and Construction 2022, CRC Press, 2023, pp. 35–42.

[43] D.I. für Normung e.V., DIN 276 Kosten im Bauwesen: Building costs, Coûts de bâtiment et de travaux publics (btp), Tech. Rep, 2018.

[44] f:data GmbH, Baupreislexikon, 2022, https://www.baupreislexikon.de, (Last accessed 27 February 2023).

[45] R. Müller, BKI Baukosten GebäUde Neubau 2020: Statistische Kostenkennwerte GebäUde (Teil 1), first ed., BKI Baukosteninformationszentrum, 2020.

[46] Nutzungsdauern von Bauteilen für Lebenszyklusanalysen nach Bewertungssystem Nachhaltiges Bauen (BNB), Federal Institute for Research on Building, Urban Affairs and Spatial Development (BBSR) at the Federal Office for Building and Spatial Development of Germany, 2011.

[47] Leitfaden Nachhaltiges Bauen - Anlage 6: Bewertung der Nachhaltigkeit von Gebäuden und Liegenschaften, Federal Office for Building and Regional Planning of Germany, 2001.

[48] CEN, Sustainability of Construction Works - Methodology for the Assessment of Performance of Buildings - Part 1: Environmental Performance; German and English Version pren 15978-1:2021 (EN15978), Tech. Rep, 2021.

[49] Federal Ministry for Housing, Urban Development and Building, Ökobaudat, 2022, https://https://www.oekobaudat.de, (Last accessed 27 February 2023).

[50] H.M. Harter, Lebenszyklusanalyse der technischen gebäudeausrüstung großer wohngebäudebestände auf der basis semantischer 3D-stadtmodelle (Ph.D. thesis), Technische Universität München, 2021.

[51] H. Harter, B. Willenborg, W. Lang, T.H. Kolbe, Life cycle assessment of building energy systems on neighbourhood level based on semantic 3D city models, J. Clean. Prod. 407 (2023) http://dx.doi.org/10.1016/j.jclepro.2023.137164.

[52] D. Eberle, F. Aicher, E. Hueber, be 2226 Die Temperatur der Architektur/The Temperature of Architecture: Portrait eines energieoptimierten Hauses/Portrait of an Energy-Optimized House, Birkhäuser, 2016.

[53] F. Nagler, Einfach Bauen: Ein Leitfaden, Birkhäuser, 2021.

[54] L. Diao, Y. Sun, Z. Chen, J. Chen, Modeling energy consumption in residential buildings: A bottom-up analysis based on occupant behavior pattern clustering and stochastic simulation, Energy Build. 147 (2017) 47–66.

[55] J. Rouleau, L. Gosselin, P. Blanchet, Robustness of energy consumption and comfort in high-performance residential building with respect to occupant behavior, Energy 188 (2019) 115978.

[56] Federal statistical office of Germany, Statistisches bundesamt, 2023, https://www.destatis.de/DE/Home/_inhalt.html, (Last accessed 1 March 2023).

[57] The statistical office of the European Union, Eurostat, 2023, https://ec.europa.eu/eurostat/web/main/home, (Last accessed 5 March 2023).

[58] F. Banihashemi, M. Weber, W. Lang, Model order reduction of building energy simulation models using a convolutional neural network autoencoder, Build. Environ. 207 (2022) 108498.

[59] X. Chen, P. Geyer, Machine assistance in energy-efficient building design: A predictive framework toward dynamic interaction with human decision-making under uncertainty, Appl. Energy 307 (2022) 118240.

[60] T. Duan, A. Anand, D.Y. Ding, K.K. Thai, S. Basu, A. Ng, A. Schuler, Ngboost: Natural gradient boosting for probabilistic prediction, in: International Conference on Machine Learning, PMLR, 2020, pp. 2690–2700.

[61] MHCLG, Energy performance of buildings data: England and Wales, Ministry of Housing, Communities and Local Government (MHCLG, 2020.

[62] M. Kottek, J. Grieser, C. Beck, B. Rudolf, F. Rubel, World map of the Köppen-Geiger climate classification updated, 2006.

[63] F. Rubel, K. Brugger, K. Haslinger, I. Auer, et al., The climate of the European Alps: Shift of very high resolution Köppen-Geiger climate zones 1800–2100, Meteorol. Z. 26 (2) (2017) 115–125.
[64] A. Shapiro, Monte Carlo sampling approach to stochastic programming, in: ESAIM: Proceedings, Vol. 13, EDP Sciences, 2003, pp. 65–73.
[65] A. Shapiro, Stochastic Programming By Monte Carlo Simulation Methods, Humboldt-Universität zu Berlin, Mathematisch-Naturwissenschaftliche Fakultät ..., 2000.
[66] R. Jiang, Y. Guan, Risk-averse two-stage stochastic program with distributional ambiguity, Oper. Res. 66 (5) (2018) 1390–1405.
[67] Deutsches Institut für Normung e.V., DIN V-4701-10 Kosten im Bauwesen: Building costs, Coûts de bâtiment et de travaux publics (btp), Tech. Rep, 2003.
[68] eurostat, Energy consumption in households, 2023, https://ec.europa.eu/eurostat/statistics-explained/index.php?title=Energy_consumption_in_households#Energy_consumption_in_households_by_type_of_end-use, (Last accessed 22 March 2023).
[69] J. Blank, K. Deb, pymoo: Multi-objective optimization in Python, IEEE Access 8 (2020) 89497–89509.
[70] B. Palacios-Munoz, B. Peuportier, L. Gracia-Villa, B. López-Mesa, Sustainability assessment of refurbishment vs. new constructions by means of LCA and durability-based estimations of buildings lifespans: A new approach, Build. Environ. 160 (2019) 106203.
[71] C. Thibodeau, A. Bataille, M. Sié, Building rehabilitation life cycle assessment methodology–state of the art, Renew. Sustain. Energy Rev. 103 (2019) 408–422.
[72] Federal statistical office of Germany, Consumer price index, 2023, https://www.destatis.de/DE/Themen/Wirtschaft/Preise/Verbraucherpreisindex/aktuell-energie.html, (Last accessed 1 August 2023).